

### Central European Journal of Chemistry

# Spectral properties of coumarin derivatives in various environments

#### Research Article

Alzbeta Holubekova\*, Pavel Mach, Jan Urban

Faculty of Mathematics, Physics and Informatics, Comenius University, 842 48 Bratislava, Slovakia

#### Received 31 July 2012; Accepted 5 November 2012

Abstract: The structural and spectral properties of coumarin derivatives in complex environments were investigated within the time-dependent density functional theory (TD DFT). Absorption spectra calculations were obtained at TD PBE0/6-31+G(d,p) level of theory for coumarin47 in the gas-phase and in various polar and non-polar organic solvents. The geometries of coumarins 6, 30, 47 and 522 in the gas phase and in inclusion complexes with the β-cyclodextrin (βCD) were determined by PM3 and DFT (HCTH/6-31G) calculations. Encapsulation of coumarin in βCD and associated changes in electronic structure produced either a red or blue shift in the absorption spectra of coumarins. A proposed cavity model for βCD-coumarin complex in water solution allowed identification of various contributions to the overall shift in the absorption spectra of coumarin upon complex formation in a solvent environment.

**Keywords:** TD DFT • Coumarins •  $\beta$ -cyclodextrin • Absorption spectra © Versita Sp. z o.o.

## 1.Introduction

Coumarin derivatives (derived from the basic structure of coumarin by means of substitution, Fig. 1) having wide range of size, shape and hydrophobicity, represent useful fluorescent probes of heterogeneous environments, such as supramolecular host cavities (e.g. cyclodextrins), surfactants related mesostructures (e.g. micelles [1] and Langmuir-Blodgett layers [2]), micro- and nanoparticles of solids [3], as well as polymers [4]. Inclusion complexes of these molecules with cyclodextrins present an interesting subject to study. Experimental methods can be used to gain insight into complex formation and the position of the guest molecule in the cyclodextrin cavity. The evidence of inclusion complexes of β-cyclodextrin (βCD) and guest molecule was obtained using X-ray crystallography [5-7]. Also UV-VIS, FTIR, NMR spectroscopy, differential scanning calorimetry and electrochemical methods have been used to study CDs and their inclusion complexes [6,8-19].

Various contributions to the complex stability can be summarized according to the role they play in the complex formation. It was found that van der Waals interaction and hydrophobic interaction constitute the major driving forces for cyclodextrin complexation, whereas electrostatic interaction and hydrogen bonding can significantly affect the conformation of particular inclusion complex [20]. A computational approach provides insight in the interaction of a guest molecule with  $\beta$ CD, the structure of the complex, to find the preferred orientation of guest in the cavity.

Spectral characteristics of coumarins can be used to test various properties of cyclodextrins. Even though the last few decades have brought an increase in the capability of theoretical methods, the calculation of spectroscopic properties of βCD-coumarin inclusion complexes is still impractical. Despite this fact, coumarins present a very interesting group of molecules for theoretical study. Earlier studies used semi-empirical methods [21,22], that have been shown to be less accurate as they were only able to yield qualitative predictions of spectral characteristics. Configuration interaction-singles (CIS) as well as the TD DFT were applied and the comparison of accuracy of both methods for the calculation of coumarin spectral properties was provided in several studies [23-25]. Since TD DFT provides a very reliable compromise between computational cost and accuracy it is widely used for the calculation of spectral properties of coumarins

$$CH_{3}CH_{2}N$$

$$CH_{3}CH_{2}$$

$$CH_$$

Figure 1. Coumarin derivatives.

coumarin522

[26-28]. To obtain results from calculations which are comparable to experimental studies, the solvent effect has to be taken into account, either by the use of an explicit or implicit solvent model. The most convenient way to incorporate the solvent effects implicitly into a CIS or TD DFT calculation is the Polarizable Continuum Model (PCM) [24,29-31] Although its implementation in calculations usually increases the accuracy of the spectral wavelengths obtained, it may not be sufficient in some cases to obtain results with quantitative predictive strength [32,33].

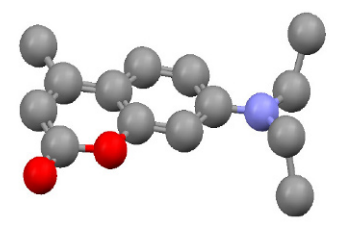
The primary objective of our paper is to provide a picture of the spectral properties of selected coumarin derivatives in the gas phase, in the solution phase and in the complexes with  $\beta$ -cyclodextrin. The paper

is organized as follows: section 2 gives the methods used for the calculation of the structures of coumarins and  $\beta CD$ -coumarin inclusion complexes and spectra calculations. The results are presented in the third section with the emphasis to evaluation of the spectral characteristics of coumarin47; including absorption spectra, emission spectra, solvatochromic shift and Stokes shift, also the results of cavity model of  $\beta CD$ -coumarin47 complexes in water are presented. Finally, the conclusions of the results obtained summarize the paper.

## 2. Calculation details

The βCD input structure for the calculation was taken from the Cambridge Crystallographic Database [34]. The structures of coumarin6 (c6), coumarin30 (c30), coumarin47 (c47) and coumarin522 (c522) were constructed using Hyperchem code [35]. Each molecule was optimized at the PM3 [36,37] level of theory and the structure with lowest energy has been chosen to build the complex with βCD. The input structure of the βCDcoumarin complex was formed in the following way: BCD was placed at the origin of a coordinate system and coumarin was put on the edge of secondary rim and passed through the cavity by steps. The step length was 0.1 Å. In each step four angles were optimized which characterize the relative position of coumarin and βCD. The same approach was carried out with the coumarin entering the cavity from the opposite side. After that the lowest energy conformation was optimized without any restrictions. The geometries of PM3 fully optimized complexes were used for the calculations at the DFT level of theory (HCTH method [38]) using 6-31G basis set. The gas phase geometries of coumarins were optimized at the PM3 and DFT level (functionals HCTH [38], PBE0 [39] and B3LYP [40,41,42]) with two basis sets (6-31G and 6-31+G(d,p)).

To see the influence of complex formation on spectra the absorption maxima of coumarins and  $\beta CD$ -coumarin complexes were estimated. Calculations were performed at CIS/6-31G, HCTH/6-31G, PBE0/6-31G levels of theory. In the case of c47 larger basis set was used, namely calculations were done on PBE0/6-31+G(d,p) level. In order to separate the effect of geometry change on spectra upon encapsulation we evaluated the gas-phase spectra of coumarins in the complex conformation (geometry of coumarin molecule corresponding to that in the complex) at PBE0/6-31G level. For c47 the absorption maximum in complex geometry was also calculated using the 6-31+G(d,p) basis set.



Conformer A

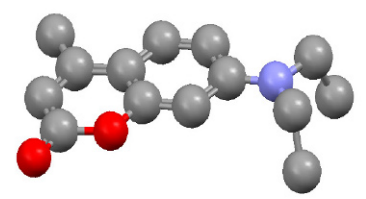


Figure 2. Conformers of coumarin47 (Hydrogens are omitted for clarity).

Additionally, the spectra calculations were performed on B3LYP/6-31+G(d,p) optimized structures of coumarins. The spectral properties of coumarin molecules were obtained at the TD DFT level of the theory using the PBE0 hybrid functional and 6-31+G(d,p) basis set as a reasonable compromise between precision and computational costs. For the two smaller molecules (c47 and c522) we evaluated the spectra at CC2/aug-cc-pvDZ and CC2/def2-TZVPP levels of theory in both cases taking advantage of Resolution of Identity (RI) approximation [43].

Spectral properties (maximum absorption wavelength, solvatochromic shift, dynamic and static Stokes shift) were evaluated for c47 in solvents (water, acetonitrile, methanol, tetrahydrofuran, chloroform, ether, toluene, cyclohexane and heptane). The solvent effects were implemented in the calculation *via* the PCM model [44] in its IEF version [45] as implemented in GAUSSIAN03.

The experimental Stokes shift for a molecule in solution can be divided in static Stokes shift resulting from atomic relaxation of solute and dynamic Stokes shift arising due to the reorganization of solvent molecules in the environment of the excited molecule. In spite of the simplicity of this model it captures two basic physical processes during the molecular excitation and de-excitation in solvent.

To test the ability of theoretical treatment on dynamic Stokes shift of coumarins we have used coumarin153 (c153) as a benchmark molecule. We have chosen this molecule because due to its simple solvatochromic behaviour it is often used as a solvation dynamics probe

in experimental studies. Therefore a number of papers have been published on experimental measurements of the spectral characteristics of coumarin153 in various solvents; see e.g. [46,47,48]. We used the results published by Maroncelli et al. [46] as benchmark data. To evaluate the dynamic Stokes shift the calculations of excitation energies in solvents have been performed within the equilibrium approximation. The difference between excitation energies calculated by using the non-equilibrium and equilibrium solutions provided a measure of dynamic Stokes shift.

A detailed study of spectral properties has been performed for coumarin47. Two conformers, A and B (Fig. 2), were optimized using B3LYP/6-31+G(d,p) in vacuum and the optimized structures were used for all absorption spectra calculations. The two conformers differ in the conformation of the diethylamino substituent. The terminal methyl groups of the diethylamino group are oriented either to a different side of the coumarin mean plane (conformer A) or to the same side (conformer B). The geometries were optimized at the B3LYP/6-31+G(d,p) level. The gas-phase absorption spectra were calculated at different levels of theory (CIS/def2-TZVPP, CIS/aug-cc-pvDZ CIS/6-31+G(d,p), TD DFT (PBE0/6-31+G(d,p), CC2/def2-TZVPP and CC2/augcc-pvDZ). Factor 0.72 proposed by Broo and Holmen [49] was used to scale the results calculated with the CIS method. The dynamic Stokes shift was evaluated as described above. Additionally, the static Stokes shift was estimated as the difference between the excitation energies calculated within the nonequilibrium approach and the emission energies calculated by using the equilibrium solutions. Upon addition of calculated dynamic and static Stokes shift values, we obtained data comparable to the experimental values of the Stokes shift.

A cavity model was proposed for the  $\beta$ CD-coumarin47 complex. It was built on the HCTH optimized geometry of the complex. The cavity was constructed to replace the  $\beta$ CD. Twelve dummy atoms were placed at the distance d=5.36 Å from the  $\beta$ CD mean axis in a cylindrical arrangement, six on both sides of  $\beta$ CD mean plane at the distance l=1.5 Å. The van der Waals radius on the dummy atoms was increased stepwise from r=2.8 Å up to r=4.2 Å. Corresponding absorption maxima of coumarin47 in the cavity were estimated and the solvent effect of water was included using PCM.

Principally, the calculations have been carried out with the GAUSSIAN03 package of programs [50] applying default procedures and parameters. The CC2 calculations of spectral and electrical properties have been performed in Turbomole version 5-10 [51].

Table 1. Angle between the coumarin mean plane and benzoimidazole (for c30) or benzothiazole (for c6) mean plane. Values are in [deg].

	РМЗ		HCTH/6-31G		PBE0/6-31G	B3LYP/6-31+G(d,p)
	gas-phase	complex	complex	gas-phase	gas-phase	gas-phase
c30	54.76	55.72	49.14	38.86	35.12	41.75
с6	82.02	86.86	0.93	18.83	16.63	34.27

Table 2. Stabilization energy of complexes, values are in [eV].

Complexation energy	РМЗ	HCTH/6-31G
C6	0.676	1.045
C30	0.529	0.763
C47	1.062	0.798
C522	0.464	0.477

## 3. Results and discussion

#### 3.1. Structural properties

No significant changes concerning the bond lengths were observed upon complex formation. The differences in the coumarin geometry were mainly caused by the bond angles changes. Gas phase optimizations revealed a planar structure of the coumarin moiety. Slight distortion in the planarity of the coumarin moiety after encapsulation was observed at HCTH/6-31G level for all coumarin derivatives and for c30, c6 and c47 at the PM3 level. The distortion of planarity was the most pronounced in case of PM3 optimized complex with c522 and the geometry of coumarin moiety became "twisted". This indicates that the PM3 method did not describe dispersion interactions properly. The PM3 optimization yielded geometries with a pyramidalized nitrogen atom in the diethylamino substituent for c6 and c30 in gas-phase and in the complex. The originally planar structure of c47 changed to pyramidalized after formation of the complex. In contrast, optimizations at the DFT level estimated an almost planar geometry for the nitrogen atom in the diethylamino substituent in all coumarins before and after formation of the complex.

In case of c6 and c30, results of all optimizations confirmed planar benzothiazole and benzoimidazole moieties. Since these substituents were located outside the  $\beta$ CD cavity, their geometry did not change upon complexation. However the angle between the benzothiazole or benzoimidazole moiety and the coumarin moiety differed for various methods (Table 1). The relative position of the substituent and coumarin moiety changed mainly by rotating the substituent along the bond connecting them.

The PM3 gas-phase optimization of  $\beta$ CD yielded a symmetric structure of the molecule. After the

optimization with HCTH/6-31G the symmetry of  $\beta$ CD increased. The conical shape of  $\beta$ CD became more cylindrical and simultaneously the number of stabilizing hydrogen bonds between the hydroxyls on the secondary rim and between the OH groups and the O of the adjacent glucose unit on the primary rim increased.

The structure of βCD upon complex formation calculated with PM3 changed only slightly. The general shape remained the same; an additional hydrogen bond between the secondary hydroxyl groups was formed for the complexes with c6 and c47. The complex formation calculated at PM3 level showed a more pronounced effect on the geometries of coumarins. Contrary to PM3 optimized complexes, the HCTH optimizations led to deformation in the βCD symmetry. The gas phase symmetrical arrangement of glucose units became distorted by adapting the cavity to the shape of the inserted coumarin molecule (Fig. 3). After complexation the hydrogen bonds between the hydroxyl groups remained preserved. Additional hydrogen bonds between the primary hydroxyl groups of BCD were formed in complexes with c6 and c30. Intermolecular hydrogen bonds were observed in all complexes, with the exception of that formed with c6.

The complexation energy was favourable for the complex formation (Table 2). Our calculations were carried out without solvent. Due to the hydrophobicity of coumarins it can be expected that the presence of polar solvent will further increase the complex stability.

#### 3.2. Spectral properties

Table 3 gives the results obtained for spectra calculation at different levels of theory for molecular structures obtained at the HCTH/6-31G level. TD HCTH/6-31G absorption maxima of gas-phase coumarins were significantly overestimated and it completely failed in spectra calculation for  $\beta$ CD-coumarin complexes. For this case we estimated the shift due to the complex formation by TD PBE0/6-31G and CIS/6-31G. Since the CIS values were underestimated we scaled them by factor 0.72. Both methods agreed qualitatively well. A red shift was observed for c47, c6 and c522 upon encapsulation of coumarin in  $\beta$ CD. In contrast, the c30 absorption maximum was blue shifted. To see the origin for this effect we estimated the spectra of gas-phase

coumarin in the complex conformation. This calculation revealed that the shift due to the geometry difference for c30 ( $\Delta v_{geom}$  = -761 cm<sup>-1</sup>) was in the opposite direction compared to other coumarins. The shift  $\Delta v_{geom}$  was small for c47 and c522 (51 cm<sup>-1</sup> and 37 cm<sup>-1</sup>, respectively); these molecules are relatively small and rigid in comparison to c6 and c30 and their geometry changed only slightly after the encapsulation. In the case of c6, the most significant difference in geometry

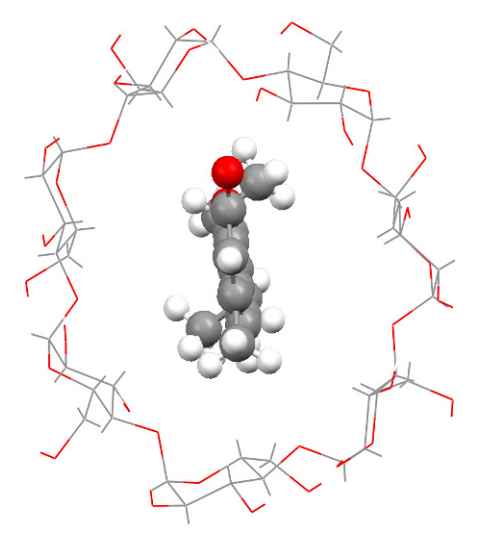


Figure 3. HCTH optimized βCD-coumarin47 complex.

after encapsulation was that the angle between benzothiazole and coumarin moiety became only 0.93°. The resulting extension of  $\pi$  electron system caused red shift  $\Delta v_{geom}=430~\text{cm}^{-1}.$  The shift due to  $\beta\text{CD}$  presence  $(\Delta v_{cmplx}-\Delta v_{geom})$  was always red and approximately 700 - 900 cm $^{-1}$  for c6, c30 and c47. For c522 the shift was the most pronounced. It seems likely that the size of the  $\beta\text{CD}$  cavity did not facilitate the inclusion of c552 in comparison to other coumarins. Thus the overall shift due to the complexation was a combination of the above mentioned contributions  $(\Delta v_{geom}$  and  $\Delta v_{\beta\text{CD}})$  and could be in both directions, according to the substituent groups on coumarins and the extent of geometrical changes on involved molecules upon inclusion.

The absorption spectra calculated on B3LYP/6-31+G(d,p) geometries are listed in Table 4. The value of CC2/def2-TZVPP maximum absorption wavelength can be used as a reference value to estimate the accuracy of the PBE0 functional. These results show that even though PBE0/6-31+G(d,p) put the lowest demand on computational time, it still provided results with satisfactory accuracy in comparison to higher level theory calculations. The last row in Table 4 lists the shift between absorption spectra calculated at the same level (PBE0/6-31+G(d,p)) but on different geometries (HCTH/6-31G and B3LYP/6-31+G(d,p)). Although, the change in geometry by optimization at different

Table 3. Absorption maxima calculated for complexes and gas phase coumarins on HCTH/6-31G geometries. Values reported are in [cm<sup>-1</sup>].

Method	Geometry	c47	<b>c</b> 6	c30	c522
HCTH/6-31G	gas-phase	25877	22578	21789	22916
CIS/6-31G	gas-phase	39213	33371	34875	35741
	complex	38643	31925	35174	35112
scaled CIS/6-31G	gas-phase	28233	24027	25110	25733
	complex	27823	22986	25325	25281
	$\Delta v_{ ext{cmplx}}$ (scaled)	411	1041	-216	453
PBE0/6-31G	gas-phase	30078	25574	26314	26579
	complex	29137	24391	26366	25510
	$\Delta {f v}_{ m cmplx}$	941	1183	-53	1070
	gas-phase (complex geometry)	30027	25145	27075	26542
	$\Delta {\sf v}_{\sf geom}$	51	430	-761	37
	$\Delta V_{ m eta CD}$	891	753	708	1033
PBE0/6-31+G(d,p)	gas-phase	29464	24848	25417	26243
	complex	28797			
	$\Delta {f v}_{ m cmplx}$	667			
	gas-phase (complex geometry)	29394			
	$\Delta { m v}_{ m geom}$	69			
	$\Delta v_{f BCD}$	598			

Table 4. Absorption maxima of gas-phase-coumarins on B3LYP geometry. Δν<sub>GEOM</sub> is the shift between the absorption maxima calculated on different geometries (HCTH/6-31G and B3LYP/6-31+G(d,p)) at TD PBE0/6-31+G(d,p) level. Values are reported in [cm<sup>-1</sup>].

Method	c47	с6	c30	c522
PBE0/6-31+G(d,p)	30287	26349	26494	27700
PBE0/TZVPP	30349	26319	26403	27809
CC2/TZVPP	30586			27889
CC2/aug-cc-pvDZ	30295			27729
$\Delta \mathbf{v}_{\mathbf{GEOM}}$	823	1501	1077	1457

**Table 5.** Gas phase maximum absorption wavelength of coumarin47 for conformers A and B. For CIS calculation the scaled values are reported in parenthesis.

Method/basis set		[cm <sup>-1</sup> ] Conformer B	
CIS/def2-TZVPP	39111 (28160)	39134 (28176)	
CIS/aug-cc-pvDZ	38764 (27910)	38782 (27923)	
CIS/6-31+G(d,p)	39148 (28187)	39165 (28199)	
TD DFT (PBE0/6-31+G(d,p) )	30287	30346	
CC2/def2-TZVPP	30586	30678	
CC2/aug-cc-pvDZ	30295	30358	

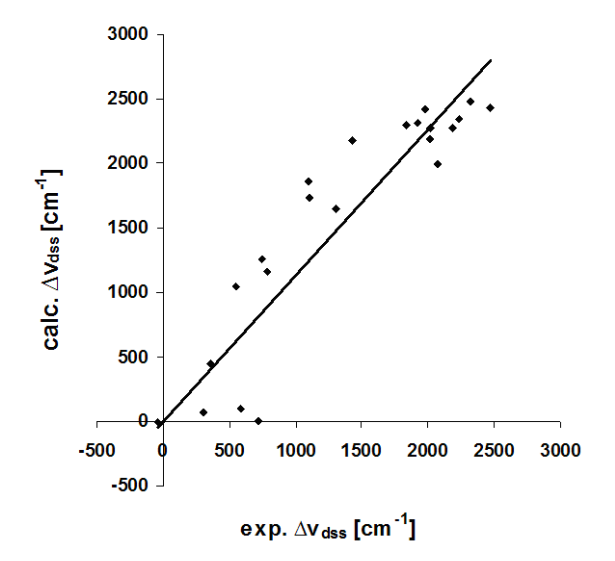


Figure 4. Comparison of theoretically (PBE0/6-31+G(d,p)) and experimentally [46] estimated dynamic Stokes shift Δν<sub>dss</sub> [cm<sup>-1</sup>] for c153. The line represents the correlation of data (slope=1.13, R²=0.82).

DFT levels (HCTH/6-31G and B3LYP/6-31+G(d,p)) did not reveal a significant difference in bond lengths and angles (only that the smaller basis preferred the more planar structures), the overall summation of various small contributions led to absorption maxima shift  $\Delta v_{\text{GEOM}}$  = 823-1501 cm<sup>-1</sup>. The most pronounced

shift in the case of c6 could be ascribed to the different geometry of diethylamino substituent in the HCTH and B3LYP optimizations. Concerning c522, we observed a different value of pyramidalization angle depending on the basis set used to perform the optimization, which could contribute to the shift.

The calculations performed in the benchmark study on c153 confirmed the availability of TD DFT to describe the first electronic transition in coumarin molecules. The results showed that the PCM could be used to predict the absorption spectra in solvents. Although in general it underestimated the differences between solvents with various polarity, the overall trend in solvatochromic shift agreed qualitatively with experimental one. Moreover, the values of dynamic Stokes shift were in good agreement with experimental counterparts as shown in Fig. 4.

Calculations of spectral properties of c47 have been performed on two conformers. The energy gap between these two conformers was 0.028 eV with conformer A characterized by opposite orientation of ethyl groups being the lower energy conformer.

Values of gas-phase absorption maxima for both conformers are provided in Table 5. Due to the lack of dynamic electron correlation, the scaling factor 0.72 was used to scale the results obtained by CIS method. The scaled values are reported in parenthesis. In the absence of experimental data we take the CC2/ def2-TZVPP value as a reference, since the basis set incompleteness error of the def2-TZVPP basis set is small enough to obtain quantitative results at the CC2 level. The unscaled CIS results tended to overestimate the absorption wavelengths whilst the scaled CIS tended to underestimate them, even though not so drastically. Noticeably, the DFT calculations with the lowest basis set yielded absorption wavelengths near the actual CC2/def2-TZVPP values at considerably lower computational cost. In respect to the two conformers of c47, the values varied only slightly. The CIS values differed by up to 23 cm<sup>-1</sup>, the largest shift between the A and B conformer calculated at CC2/ def2-TZVPP level is 92 cm<sup>-1</sup>. Therefore, the results reported below concern only conformer A. There are experimental absorption spectra available for c47. In this work we used three different data sets published in [52] (in this work referred to as exp1), in [53] (exp2) and [54] (exp3). To see the influence of various solvents on the absorption spectra we use a plot of these versus simple reaction field

$$(f(e_0) = \frac{e_0 - 1}{e_0 + 2}).$$

Estimation of linear correlation to individual data sets allowed the comparison of theoretical and experimental

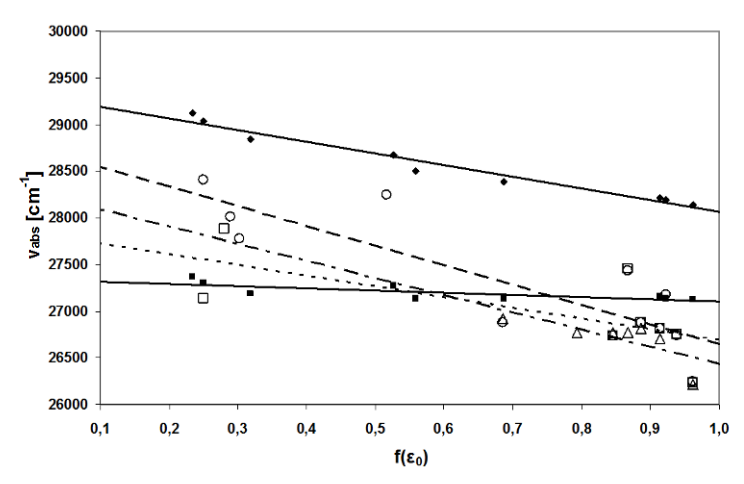


Figure 5. Maximum absorption wavelengths  $v_{abs}$  of c47 in various solvents *versus* the reaction field factor  $f(\varepsilon_0)$ . (\* TDDFT,  $\blacksquare$  CIS,  $\circ$  exp1,  $\square$  exp2,  $\Delta$  exp3, solid lines represent fits for theoretical data, long-dashed line for exp1, dotted line for exp2, dotted and dashed line for exp3).

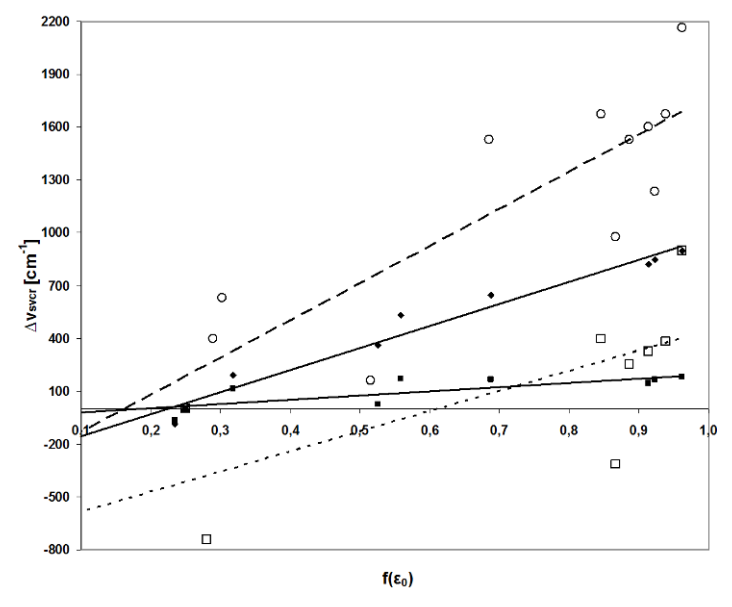


Figure 6. Comparison of solvatochromic shifts Δv<sub>svcr</sub> for c47 due to different levels of theory and experiments plotted as a function of the reaction field factor f(ε<sub>0</sub>). (♦ TDDFT, ■ CIS, ∘ exp1, □ exp2, solid lines represent fits for theoretical data, long-dashed line for exp1, dotted line for exp2).

data. The results are shown in Fig. 5. The values of TD DFT maximum absorption wavelength were overestimated in comparison to experimental values, but the overall trend of the results was satisfactory. The slopes of the fitting lines varied even for the experimental data being - 2109 for *exp1*, -1146 for *exp2* and -1841 for *exp3*. Our slope from the DFT calculation estimated a value of -1251, that was in good agreement with those from experiments. The CIS data have already been scaled by factor 0.72. The unscaled results showed an expected high overestimation of the absorption wavelength. Although the scaled values were closer to experimental data compared to DFT and the trend for the CIS results was correctly reproduced, the slope = -239 suggested that

this method showed only slight sensitivity to different polarity of the solvents. A more useful illustration on the performance of theoretical methods can be gained by estimation of the gas-to-solution (or solvatochromic shift). Since there were no experimental absorption data in vacuum for C47 available, we took the maximum absorption wavelength in cyclohexane as the reference value for the plot of solvatochromic shift (Fig. 6). The *exp3* data did not include absorption wavelength in cyclohexane and are not shown. As already suggested, the plot points out the ill-behaviour of CIS concerning to the solvatochromic shift. On the other hand the DFT values appeared to be in good agreement with the two different sets of experimental values (*exp1* and *exp2*).

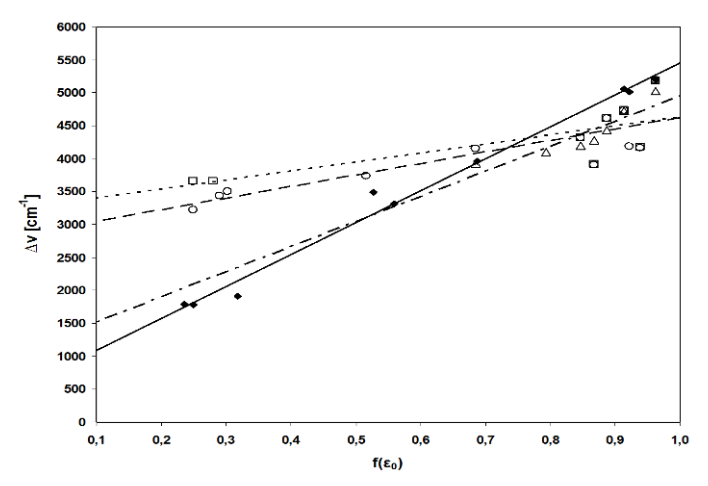


Figure 7. Theoretically and experimentally estimated Stokes shift  $\Delta v$  for c47 in solvents vs. the reaction field factor  $f(\varepsilon_0)$ . ( $\bullet$  TDDFT,  $\circ$  exp1,  $\square$  exp2,  $\Delta$  exp3, solid line represents fit for theoretical data, long-dashed line for exp1, dotted line for exp2, dotted and dashed line for exp3).

Up to now there were no experimental data on dynamic Stokes shift of c47 to be compared with our results. However our test study on coumarin153 confirmed very good correlation of theoretically and experimentally estimated dynamic Stokes shift. Upon addition of calculated dynamic and static Stokes shift values we obtained data comparable to the experimental values of the Stokes shift (Fig. 7). For the analysis we used values reported in the same papers as in the previous subsection (exp1 [52], exp2 [53] and exp3 [54]). The general trend of increasing Stokes shift with increasing solvent polarity was obvious and has been supported by the theoretical results. However, the slope of the correlation line (4855) was overestimated in comparison to experiments (1746 for exp1, 1380 for exp2 and 3809 for exp3).

As stated by Maroncelli et al. [46], the absence of hydrogen bonding in PCM does not play any significant role when dealing with protic solvents. Therefore, it is not likely that the overestimation of the slope could be ascribed to missing hydrogen bonding in theoretical approach. Moreover, the interactions in alcoholic solvents are dominated by electrostatic interactions which are correctly described by PCM. On the other hand, the description of repulsion and dispersion interactions which outweighs the electrostatic interactions in less polar solvents is merely semi-empirical. Additionally, these calculations were performed on the ground state geometry. Further optimizations of excited state (ES) structure at TD DFT level revealed that the geometry of the first excited state was close to the ground state structure. The second excited state was characterized by rotation of the diethylamino substituent. In contrast, this structure was estimated in the first excited state at CC2/ aug-cc-pvDZ level of theory. The energy gap between the first ES and second ES conformation calculated at

TD DFT level was only 0.02 eV. Therefore the difference between the ground and excited state geometry could be underestimated by calculations at the TD DFT level.

The influence of the solvent on the coumarin molecule within the cavity of  $\beta CD$  has also been studied by substitution with the cavity model. The cavity in the model should be approximately the same size as the van der Waals surface of &CD in PCM. From simple geometric consideration, taking into account the distances of atoms in ßCD and the UFF radii scaled by 1.1 used in PCM, we estimated the van der Waals radius on dummy atoms r = 3 Å as reasonable. By this value of r we obtained blue shift  $\Delta\lambda$ = 7.39 nm resulting from the change in solvent environment of coumarin due to encapsulation. Encapsulation itself produced red shift of the absorption maximum. The value was estimated to be  $\Delta\lambda$  = 7.86 nm. Since both shifts (due to the complexation and the modification of solvent environment) were in the opposite direction they would compensate each other. These results suggested that the absorption spectra of coumarin47 in water solution and &CD-coumarin complex in water are very close. Therefore the original absorption maximum of coumarin, or small blue or red shift could be observed after the complexation. To the best of our knowledge there are no experimental studies on absorption spectra of the \( \mathbb{GCD-coumarin47 complex. \) However studies on other coumarins suggest that all these alternatives are possible for coumarin derivatives encapsulated in the &CD (no shift in study on coumarin [55], 5-8 nm blue shift in case of 7-diethylaminocoumarin-3-carboxylic acid [56], 4 nm red shift for coumarin120 [57]). Thus, even qualitative prediction of spectral change after complexation could be difficult. Nevertheless this model enables a closer look at various contributions to the shift of absorption maxima upon complex formation.

# 4. Conclusions

In the present work we have explored the spectral properties of coumarin derivatives in environments: in vacuum, in inclusion complexes with  $\beta$ CD and in solution. The results showed that  $\beta$ CD was able to encapsulate coumarin molecules inside its cavity and that the complexes were stabilized by intermolecular hydrogen bonding. Calculations of maximum absorption wavelengths performed on gas-phase coumarins and complexes revealed a red shift upon complexation for coumarins c47, c6 and c522. In contrast, the complex formation of coumarin30 resulted in a blue shift. Further spectra calculations on coumarin structures corresponding to the geometry of the coumarin molecule complexed by BCD revealed that the shift between various geometry structures (gas-phase and that in the complex) can be in both directions. The value of this shift depended on the rigidity of the molecule, substituent groups and depth of inclusion of the particular coumarin molecule. The shift due to the presence of βCD was always red. Although the HCTH functional was used for geometry optimizations and provided reliable structures of BCD-coumarin complexes it failed in calculation of absorption maxima for the complexes. By proposing the cavity model of BCD-coumarin complex the value of the shift upon encapsulation of coumarin47 in βCD in water environment was found to be reasonable.

The benchmark study on coumarin153 confirmed the semi-quantitative reliability of TD DFT/PCM calculation with the PBE0 functional for spectral properties evaluation. Calculations of dynamic Stokes shift and comparisons with experimental values confirmed good agreement.

References

- [1] N.C. Maiti, M.M.G. Krishna, P.J. Britto, N. Periasamy, J. Phys. Chem. B 101, 11051 (1997)
- [2] K. Ray, A.K. Dutta, T.N. Misra, J. Lumin. 71, 123 (1997)
- [3] J. Panyam, S.K. Sahoo, S. Prabha, T. Bargar, V. Labhasetwar, Int. J. Pharm. 262, 1 (2003)
- [4] C.D. Grant, M.R. DeRitter, K.E. Steege, T.A. Fadeeva, E.W. Castner, Langmuir 21, 1745 (2005)
- [5] J.A. Hamilton, L.K. Steinrauf, Acta Crystallogr. 24, 1560 (1968)
- [6] D. Haiyun, C. Jianbin, Z. Guomei, S. Shaomin, P. Jinhao, Spectrochim. Acta A 59, 3421 (2003)
- [7] Y. Zhang, , S. Yu, , F. Bao, Carbohydr. Res. 343, 2504 (2008)
- [8] C. Nunez-Aguero, C. Escobar-Llanos, D. Diaz,

We have computed the absorption and emission spectra of coumarin47 in gas-phase and various solvents using a PCM/TD PBE0/6-31+G(d,p) approach. Calculation of the absorption spectra were additionally carried out at CIS/6-31+G(d,p) level of theory. By comparison of the absorption maxima to experimental results we found that the TD DFT outperformed the CIS method. Evaluation of the Stokes shift at TD DFT level and comparison to experimental counterparts confirmed that the general trend of increasing Stokes shift with increasing solvent polarity was obvious and has been supported by the theoretical results. Optimizations of the excited state structure at two different levels of theory (TD PBE0/6-31+G(d,p) and CC2/aug-cc-pvDZ) identified different lowest energy conformations of c47. The proper description of excited state structure of c47 in the gas phase and in solvents with various polarities remains an objective of further investigation. The results obtained in the course of our study and presented in here suggest that DFT and TD DFT are useful for the calculation of structural and spectral properties of coumarins. Implementation of solvent effects via PCM allows direct comparison of spectral properties to experimental results. The computational demands/accuracy ratio is reasonable for investigation of supramolecular complexes with βCD.

# **Acknowledgment**

This work was sponsored by VEGA Agency Grant No 1/0524/11

- C. Jaime, R. Garduno-Juarez, Tetrahedron 62, 4162 (2006)
- [9] A. Bernini, O. Spiga, A. Ciutti, M. Scarselli, G. Bottoni, P. Mascagni, N. Niccolai, Eur. J. Pharm. Sci. 22, 445 (2004)
- [10] X. Wen, F. Tan, Z. Jing, Z. Liu, J. Pharm. Biomed. Anal. 34, 517 (2004)
- [11] M.B. de Jesus, L. de Matos Alves Pinto, L.F Fraceto, Y. Takahata, A.C.S. Lino, C. Jaime, E. de Paula, J. Pharm. Biomed. Anal. 41, 1428 (2006)
- [12] C.W. Lee, S.J. Kim, Y.S. Youn, E. Widjojokusumo, Y.H. Lee, J. Kim, Y.W. Lee, R.R. Tjandrawinata, J. Supercrit. Fluids 55, 348 (2010)
- [13] D. Bonenfant, P. Niquette, M. Mimeault, A. Furtos-Matei, R. Hausler, Water Res. 43, 3575

(2009)

- [14] A. Abou-Okeil, A. El-Shafie, Carbohydr. Polym. 84, 593 (2011)
- [15] E. Ziemons, G. Dive, B. Debrus, V. Barillaro, M. Frederich, R. Lejeune, L. Angenot, L. Delattre, L. Thunus, Hubert P, J. Pharm. Biomed. Analysis. 43, 910 (2007)
- [16] V. Harabagiu, B.C. Simionescu, M. Pinteala,
   C. Merrienne, J. Mahuteau, P. Guegan,
   H. Cheradame, Carbohydr. Polym. 56, 301 (2004)
- [17] F. Jara, M. Dominguez, M.C. Rezende, Tetrahedron 62, 7817 (2006)
- [18] M.B. de Jesus, L. de Matos Alves Pinto, L.F Fraceto, Y. Takahata, A.C.S. Lino, C. Jaime, E. de Paula, J. Pharm. Biomed. Anal. 41, 1428 (2006)
- [19] J.S. Holt, J. Mol. Struct. 965, 31 (2010)
- [20] L. Liu, Q.X. Guo, J. Incl. Phenom. Macrocycl. Chem. 42, 1 (2002)
- [21] M. Hillebrand, S. Ionescu, Chem. Phys. 293, 53 (2003)
- [22] V.K. Sharma, P.D. Saharo, N. Sharma, R.C. Rastogi, S.K. Ghoshal, D. Mohan, Spectrochim. Acta A 59, 1161 (2003)
- [23] T. Tsuji, M. Onoda, Y. Otani, T. Ohwada, T. Nakajima, K. Hirao, Chem. Phys. Lett. 473, 196 (2009)
- [24] D. Jacquemin, E.A. Perpète, X. Assfeld, G. Scalmani, M.J. Frisch, C. Adamo, Chem. Phys. Lett. 438, 208 (2007)
- [25] J. Preat, D. Jacquemin, V. Wathelet, J.M. André, E.A. Perpète, J. Phys. Chem. A 110, 8144 (2006)
- [26] K. Deuk Seo, H. Min Song, M. Jun Lee, M. Pastore, C. Anselmi, F. De Angelis, M.K. Nazeeruddin, M. Gräetzel, H. Kyu Kim, Dyes Pigm. 90, 304 (2011)
- [27] D. Jacquemin, A. Planchat, C. Adamo, Benedetta Mennucci, J. Chem. Theory Comput. 8, 2359 (2012)
- [28] R. Sánchez-de-Armas, M. A. San-Miguel, J. Oviedo, J. F. Sanz, Phys. Chem. Chem. Phys. 14, 225 (2012)
- [29] B. Xu, J. Yang, X. Jiang, Y. Wang, H. Sun, J. Yin, J. Mol. Struct. 917, 15 (2009)
- [30] T. Sakata, Y. Kawashima, H. Nakano, Int. J. Quantum. Chem. 109, 1940 (2009)
- [31] W. Zhao, Y. Ding, Q. Xia, J. Comput. Chem. 32, 545 (2011)
- [32] J.A. Key, S. Koh, Q.K. Timerghazin, A. Brown, C.W. Cairo, Dyes Pigm. 82, 196 (2009)

- [33] W. Zhao, W. Bian, J. Mol. Struct. 859, 73 (2008)
- [34] F.H. Allen, Acta Crystallogr. 58, 380 (2002)
- [35] HyperChem(TM) Professional 7.51 (Hypercube, Inc., 1115 NW 4th Street, Gainesville, Florida 32601, USA, 2002)
- [36] J.J.P. Stewart, J. Comput. Chem. 10, 209 (1989)
- [37] J.J.P. Stewart, J. Comput. Chem. 10, 221 (1989)
- [38] A.D. Boese, N.C. Handy, J. Chem. Phys. 114, 5497 (2001)
- [39] C. Adamo, V. Barone, J. Chem. Phys. 110, 6158 (1999)
- [40] A.D. Becke, Phys. Rev. A 38, 3098 (1988)
- [41] C. Lee, W. Yang, R.G. Parr, Phys. Rev. B. 37, 785 (1988)
- [42] A.D. Becke, J. Chem. Phys. 98, 5648 (1993)
- [43] C. Hättig, F. Weigend; J. Chem. Phys. 113, 5154 (2000)
- [44] J. Tomasi, B. Mennucci, R. Cammi, Chem. Rev. 105, 2999 (2005)
- [45] M. Cossi, G. Scalmani, N. Rega, and V. Barone, J. Chem. Phys. 117, 43 (2002)
- [46] M. Maroncelli, L. Reynolds, M.L. Horng, J.A. Gardecki, S.J.V. Frankland, J. Phys. Chem. 100, 10337 (1996)
- [47] M. Maroncelli, G.R. Fleming, J. Chem. Phys. 86, 6221 (1987)
- [48] M. Maroncelli, M.L. Horng, J.A. Gardecki, A. Papazyan, J. Phys. Chem. 99, 17311 (1995)
- [49] A. Broo, A. Holmén, J. Phys. Chem. A. 101, 3589 (1997)
- [50] M.J. Frisch, et al., Gaussian 03, Revision D. 02 (Gaussian, Inc., Wallingford, CT, 2004)
- [51] R. Ahlrichs, M. Bar, M. Haser, H. Horn, C. Kolmel, Chem. Phys. Lett. 162,165 (1989)
- [52] M.S. Zakerhamidi, A. Ghanadzadeh, M. Moghadam, Spectrochim. Acta A 78, 961 (2011)
- [53] M.S. Zakerhamidi, A. Ghanadzadeh, H. Tajalli, M. Moghadam, M. Jassas, R. Hosseini, Spectrochim. Acta A 77, 337 (2010)
- [54] T. López Arbeloa, F. López Arbeloa, M.J. Tapia,I. López Arbeloa, J. Phys. Chem. 97, 4704 (1993)
- [55] S. Bakkialakshmi, T. Menaka, Rec. Res. Sci. Tech. 2, 58 (2010)
- [56] C. Tablet, I. Matei, E. Pincu, V. Meltzer, M. Hillebrand, J. Mol. Liq. 168, 47 (2012)
- [57] M. Nowakowska, M. Smoluch, D. Sendor, J. Incl. Phenom. Macrocycl. Chem. 40, 213 (2001)